



Radio Frequency Spectroscopy of a Strongly Imbalanced Feshbach-Resonant Fermi Gas

Citation

Veillette, Martin, Eun Gook Moon, Austen Lamacraft, Leo Radzihovsky, Subir Sachdev, and D. E. Sheehy. 2008. Radio frequency spectroscopy of a strongly imbalanced Feshbach-resonant Fermi gas. *Physical Review A* 78(3): 033614.

Published Version

doi:10.1103/PhysRevA.78.033614

Permanent link

<http://nrs.harvard.edu/urn-3:HUL.InstRepos:7470490>

Terms of Use

This article was downloaded from Harvard University's DASH repository, and is made available under the terms and conditions applicable to Open Access Policy Articles, as set forth at <http://nrs.harvard.edu/urn-3:HUL.InstRepos:dash.current.terms-of-use#OAP>

Share Your Story

The Harvard community has made this article openly available.
Please share how this access benefits you. [Submit a story](#).

[Accessibility](#)

Radio frequency spectroscopy of a strongly imbalanced Feshbach-resonant Fermi gas

Martin Veillette,¹ Eun Gook Moon,² Austen Lamacraft,³ Leo Radzihovsky,⁴ Subir Sachdev,² and D. E. Sheehy⁵

¹*Department of Physics, Berea College, Berea, KY 40404*

²*Department of Physics, Harvard University, Cambridge, MA 02138*

³*Department of Physics, University of Virginia, Charlottesville, VA 22904-4714*

⁴*Department of Physics, University of Colorado, Boulder, Colorado 80309*

⁵*Department of Physics, Louisiana State University, Baton Rouge, LA 70803-4001*

(Dated: August 22, 2008)

A sufficiently large species imbalance (polarization) in a two-component Feshbach resonant Fermi gas is known to drive the system into its normal state. We show that the resulting strongly-interacting state is a conventional Fermi liquid, that is, however, strongly renormalized by pairing fluctuations. Using a controlled $1/N$ expansion, we calculate the properties of this state with a particular emphasis on the atomic spectral function, the momentum distribution functions displaying the Migdal discontinuity, and the radio frequency (RF) spectrum. We discuss the latter in the light of the recent experiments of Schunck *et al.* (Science **316**, 867 (2007)) on such a resonant Fermi gas, and show that the observations are consistent with a conventional, but strongly renormalized Fermi-liquid picture.

PACS numbers: 67.85.De, 03.75.Kk, 03.75.Ss

I. INTRODUCTION

One of the key recent developments in studies of degenerate atomic gases is the tunability of atomic interactions via a Feshbach resonance (FR). This has led to the realization of a resonantly-paired s-wave superfluid that can be tuned between the two well-studied limits of a weakly-paired Bardeen-Cooper-Schrieffer (BCS) superfluid and a strongly-paired diatomic molecular Bose-Einstein condensate (BEC) superfluid [1, 2, 3, 4, 5, 6].

The two asymptotic superfluid regimes at large positive and negative FR detunings allow a detailed quantitative description, made possible by the existence of a small gas parameter, na^3 , corresponding to the ratio of a short scattering length a to a large average particle spacing $\ell = n^{-1/3}$. In contrast, although the intermediate low temperature crossover regime is a conventional superfluid, that smoothly interpolates between the BCS and BEC limits, its quantitative description (in a broad resonance case) is hindered by strong interactions, characterized by a diverging scattering length and absence of a natural small parameter [7]. The flip side, of course, is that a diverging scattering length leaves particle spacing as the only relevant length scale, leading to a universal phenomenology of a resonant Fermi gas near a unitary point.

While earlier studies focused on the case where the populations of the two atomic species involved in pairing are equal (vanishing polarization), and thus on the nature of the superfluid phase, recent experimental and theoretical investigations have extensively explored the *imbalanced* resonant Fermi gas, extending its FR detuning phase diagram to a finite polarization [10, 11, 12, 13, 14, 15, 16, 17]. These studies have consistently found that at high polarization the state is non-superfluid, and have treated it as a simple Fermi gas. However, at low detuning the system is strongly resonantly interacting,

and a detailed description of the highly polarized normal state near the resonance remains a challenge [18].

Some light on the complex nature of the strongly-interacting normal state has been shed by a recent radio frequency (RF) spectroscopy experiment [19]. At high polarization an absence of a BEC peak on one hand and presence of a temperature-dependent spectral shift relative to the atomic line, on the other, was observed. Interpreting the latter as a pairing gap [5], taken together, these observations have been interpreted as evidence for a paired non-superfluid state. While unsurprising at finite temperature, and certainly present on the BEC side of the resonance, where the gap is set by molecular binding energy, an existence of such a state at *zero* temperature would constitute a dramatic departure from a modern understanding of possible condensed matter ground states. In particular, the only established route to a suppression of boson (Cooper pairs or diatomic molecules in the present context) superfluidity at zero temperature is through a localization of bosons by quenched disorder into a Bose glass [20], by a commensurate (e.g., imposed optical) lattice into a Mott insulator [20, 21], or by crystallization as in a case of a solid ⁴He. Since none of these mechanisms appears to be at play in the trapped dilute atomic gas studied in experiments by Schunck *et al.* [19], their observations and conclusions remain puzzling.

The interpretation of RF spectra in the strongly-interacting regime has been the subject of numerous theoretical investigations [22, 23, 24, 25, 26], but remains incomplete. The recent RF spectroscopy experiments on a strongly polarized Fermi gas [19, 27], have rekindled theoretical studies of such a system with a focus on the unitarity regime [28, 29, 30] and its strong interactions in the *normal* state [31, 32, 33, 34, 35, 36].

The purpose of the present paper is to make a case for a more conservative interpretation of the RF spectra of Refs. 19, 27, namely that a non-superfluid state of a

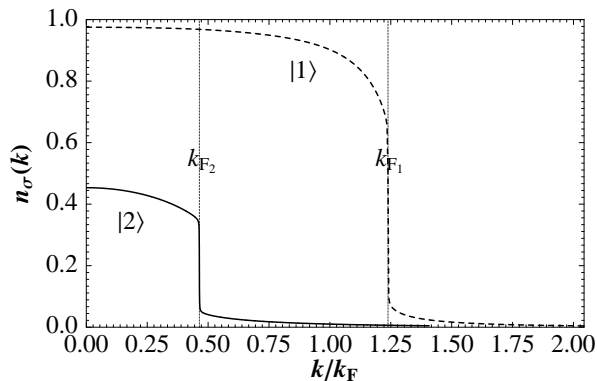


FIG. 1: Momentum distribution $n_\sigma(k)$ of the majority ($|1\rangle$) and minority ($|2\rangle$) atoms for polarization $P = 0.9$ at zero temperature and at resonance. The residues for the majority and minority atoms are, respectively, $Z_1 = 0.56$ and $Z_2 = 0.29$.

highly polarized, resonantly interacting Fermi gas is in fact a Fermi liquid, albeit a strongly renormalized one. Indeed, the Luttinger relations discussed in Refs. 37, 38 require any non-superfluid state to have Fermi surfaces for both the majority and minority species, enclosing the same volumes as for non-interacting fermions. We will show that such a Fermi liquid is perfectly consistent with the experiment of Ref. 19, and that the observed shift in the RF spectrum of the minority atoms is the result of large self-energy effects due to the Feshbach resonant scattering, as also emphasized in parallel recent studies [32, 33, 34]. Based on this we suggest that a far better test of the nature of the ground state is a measurement of the momentum distribution $n_2(k)$ of the minority atoms; in the following the label $\sigma = 1, 2$ denotes the majority and minority species, respectively. Such a measurement would be a direct test for the existence of a Fermi surface, marked by a Migdal discontinuity and characterized by the quasiparticle residues $0 < Z_\sigma < 1$

$$Z_\sigma \equiv n_\sigma(k_{F\sigma-}) - n_\sigma(k_{F\sigma+}), \quad (1)$$

illustrated in Fig. 1. This hallmark Fermi liquid feature would be absent in the case of a paired ground state, allowing for a sharp qualitative distinction between two possibilities. An interesting feature of Fig. 1 is that the functions $n_\sigma(k)$ are both universal as functions of k/k_F at resonance *i.e.* for the Fermi gas at unitarity, the functional forms (including the values of the discontinuities Z_σ) depend *only* upon the polarization P . Our computations of these universal functions is however not exact, and next we describe our computational method.

We build on our earlier studies of the superfluid state [39, 40]: our theoretical approach to the treatment of this strongly interacting (small parameter-free) normal state is based on the introduction of an artificial small parameter $1/N$, with N the number of distinct “spin”-1/2 fermion flavors in the generalized model. The advantage of such a generalization is that, for $N \rightarrow \infty$, the problem

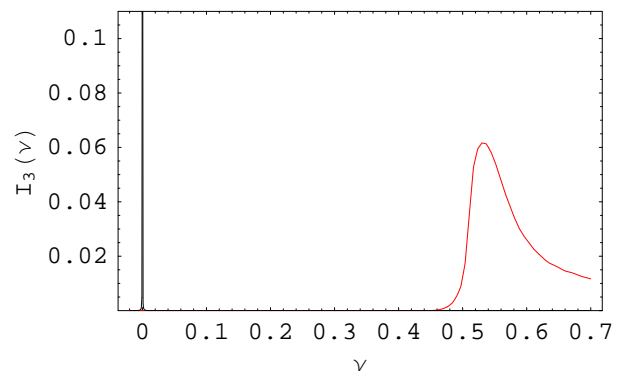


FIG. 2: RF spectrum for polarization $P = 0.97$: the intensity $I_3(\nu)$ (arbitrary units) vs. the detuning from the resonance frequency ν measured in units of the Fermi energy ϵ_F . In free space, the resonance would be at $\nu = 0$. The shift in the resonance frequency above is due to strong interactions between fermions in the non-superfluid ground state of a polarized Fermi gas. Our primary claim is that such a shift is present even while the ground state remains a Fermi liquid, with the discontinuities in the momentum distribution function shown in Fig. 1.

is exactly solvable, with finite N corrections computable via a systematic expansion in $1/N$ about this solvable limit. In particular, we calculate the RF spectrum to subleading order in $1/N$ using the full interaction matrix, including the appropriate vertex correction. We then use these controlled $1/N$ results to extrapolate to the experimentally-relevant case of a single flavor ($N = 1$) of two opposite-“spin” (hyperfine levels) fermionic atoms. This extrapolation is a subtle issue, and we cannot rule out the possibility of a nonanalyticity in the $N \rightarrow 1$ limit. However, such nonanalyticities are rare and there is no reason to expect them here.

We regard the large- N expansion as providing a framework for understanding qualitative aspects of the renormalized Fermi liquid properties of strongly-interacting imbalanced Fermi gases. A sample result for the RF spectrum obtained via this approach is shown in Fig. 2. Note the asymmetric lineshape: this arises from the imaginary part of the pairing fluctuations propagator which contains the phase space for the decay of a Cooper pair into a two fermion final state.

The universality considerations noted above for $n_\sigma(k)$ also apply to the the RF absorption spectrum. However, here there are also additional complications associated with the scattering lengths of excited states, and these will be discussed below.

The outline of the paper is as follows. In Sec. II we introduce the resonant single-channel model as well as its N -flavor generalization, and carry out its systematic expansion in $1/N$. Then, in Sec. III, we illustrate the Fermi liquid properties of the system at high polarization. In Sec. IV the radio-frequency probe is described and we discuss our results in terms of the recent experiments of Schunck *et al.*, and conclude with a brief summary in

Sec. V.

II. FORMALISM

A. Model

To capture the physics involved in the RF experiment, we model the system in terms of the three lowest hyperfine states, $|\sigma\rangle = |1\rangle, |2\rangle$ and $|3\rangle$. The two lowest states, $|1\rangle$ and $|2\rangle$, are loaded with atoms and responsible for the strong superfluid correlation, while the higher hyperfine state, $|3\rangle$, is initially empty. Experimentally, the RF field at frequency ω is used to induce atomic transitions from the state $|2\rangle$ to the state $|3\rangle$, and the induced transition rate is measured as a function of ω . As we will show below, this allows one to experimentally probe a two-particle correlation function.

Although our consideration for RF spectroscopy on fermionic atoms will be quite general, we will put particular emphasis on recent experiments on ${}^6\text{Li}$. In this system, the three lowest lying states, $|1\rangle, |2\rangle$ and $|3\rangle$ can be identified with $|F = 1/2, m_F = 1/2\rangle, |F = 1/2, m_F = -1/2\rangle$ and $|F = 3/2, m_F = -3/2\rangle$, respectively.

By integrating out the higher order hyperfine states we obtain an effective Hamiltonian in terms of the three lowest states, given by

$$\mathcal{H} = \sum_{\sigma=1}^3 \int d^3\mathbf{r} \psi_{\sigma}^{\dagger}(\mathbf{r}) \left(-\frac{\nabla_{\mathbf{r}}^2}{2m} + \bar{\omega}_{\sigma} - \mu_{\sigma} \right) \psi_{\sigma}(\mathbf{r}) + \frac{1}{2} \sum_{\sigma, \sigma'=1}^3 \int d^3\mathbf{r} \lambda_{\sigma\sigma'} \psi_{\sigma}^{\dagger}(\mathbf{r}) \psi_{\sigma'}^{\dagger}(\mathbf{r}) \psi_{\sigma'}(\mathbf{r}) \psi_{\sigma}(\mathbf{r}), \quad (2)$$

where $\lambda_{\sigma\sigma'}$ are couplings (interaction strengths set by the corresponding scattering lengths $a_{\sigma\sigma'}$) between states $|\sigma\rangle$ and $|\sigma'\rangle$. $\psi_{\sigma}^{\dagger}(\mathbf{r}), \psi_{\sigma}(\mathbf{r})$ are, respectively, the fermion creation and annihilation operators at position \mathbf{r} and hyperfine state σ , which obey the usual anticommutation relation $\{\psi_{\sigma}(\mathbf{r}), \psi_{\sigma'}^{\dagger}(\mathbf{r}')\} = \delta(\mathbf{r} - \mathbf{r}')\delta_{\sigma, \sigma'}$. The detuning of the level σ is controlled by a Zeeman field encoded by the detuning parameter $\bar{\omega}_{\sigma}$. The chemical potential μ_{σ} fixes the average atom density n_{σ} in the hyperfine state (spin) σ .

While in above model the particle number in each hyperfine state is a good quantum number, in principle there are additional interaction channels present in the physical system, that break this symmetry. For instance [41] in ${}^{40}\text{K}$, (where $|1\rangle, |2\rangle$, and $|3\rangle$ are $|F = 9/2, m_F = -9/2\rangle, |F = 9/2, m_F = -7/2\rangle$ and $|F = 9/2, m_F = -5/2\rangle$) a collision term such as $\psi_1^{\dagger}\psi_3^{\dagger}\psi_2\psi_2$ conserves the total quantum number m_F is therefore allowed by symmetry. However, effects of such interactions, that do not conserve the atom number in each hyperfine state are energetically suppressed by virtue of $2\bar{\omega}_2 \neq \bar{\omega}_1 + \bar{\omega}_3$, due to the large quadratic Zeeman splitting between the three

levels. Experimentally, the Feshbach resonances are chosen such that these kind of non-conserving processes are minimized, and therefore we will not consider them any further here.

For a short-range s-wave interaction, the Pauli principle enforces $\lambda_{\sigma\sigma} = 0$, which together with the exchange symmetry $\lambda_{\sigma\sigma'} = \lambda_{\sigma'\sigma}$, reduces the nine coupling constants $\lambda_{\sigma\sigma'}$ down to three. The corresponding three two-particle scattering lengths $a_{\sigma\sigma'}$ for atoms in states $|\sigma\rangle$ and $|\sigma'\rangle$ (for $\sigma \neq \sigma'$) are related to the strengths of the couplings $\lambda_{\sigma\sigma'}$ via the relation

$$\frac{m}{4\pi a_{\sigma\sigma'}} = \frac{1}{\lambda_{\sigma\sigma'}} + \int \frac{d^3\mathbf{k}}{(2\pi)^3} \frac{1}{2\epsilon_{\mathbf{k}}}, \quad (3)$$

where $\epsilon_{\mathbf{k}} = k^2/(2m)$ is the the free fermion dispersion.

B. Large N expansion

As discussed in the Introduction, because we are interested in the system in the vicinity of the unitary point, where the atom interaction is strong, an analysis based on a straightforward perturbation theory in the gas parameter na^3 (that diverges at the unitary point) clearly fails and an approach nonperturbative in na^3 is required. To this end, we employ the procedure, introduced and successfully utilized for the superfluid phase in Refs. 39, 40, of generalizing the physical model to that of N flavors of each of the three hyperfine states species, with the Hamiltonian given by

$$\mathcal{H} = \sum_{\sigma=1}^3 \sum_{i=1}^N \int d^3\mathbf{r} \psi_{i\sigma}^{\dagger}(\mathbf{r}) \left(-\frac{\nabla_{\mathbf{r}}^2}{2m} + \bar{\omega}_{\sigma} - \mu_{\sigma} \right) \psi_{i\sigma}(\mathbf{r}) + \frac{1}{2N} \sum_{\sigma, \sigma'=1}^3 \sum_{i, j=1}^N \int d^3\mathbf{r} \lambda_{\sigma\sigma'} \psi_{i\sigma}^{\dagger}(\mathbf{r}) \psi_{i\sigma'}^{\dagger}(\mathbf{r}) \psi_{j\sigma'}(\mathbf{r}) \psi_{j\sigma}(\mathbf{r}). \quad (4)$$

It is then straightforward to develop an expansion in powers of $1/N$, taking the physically relevant limit $N = 1$ at the end of the calculation. Since we are interested in the normal properties only, the full effective action formalism of Refs. 39, 40 will not be required. Instead we may calculate the $1/N$ contributions diagrammatically, observing that vertices bring factors of $1/N$, and particle loops a factor of N , as we sum over all components. Having thereby established the relevant class of leading $1/N$ diagrams, for ease of notation, we then drop the i flavor index.

In this way, we arrive at the thermal Green's function of species σ defined by

$$G_{\sigma}(\mathbf{k}, i\omega_n) = - \int_0^{\beta} d\tau e^{i\omega_n \tau} \langle T_{\tau} \{ \psi_{\sigma}(\mathbf{k}, \tau) \psi_{\sigma}^{\dagger}(\mathbf{k}, 0) \} \rangle, \quad (5)$$

where $\omega_n = 2\pi(n + \frac{1}{2})/\beta$ is the fermionic Matsubara frequency and $\beta = 1/T$ is the inverse temperature T and

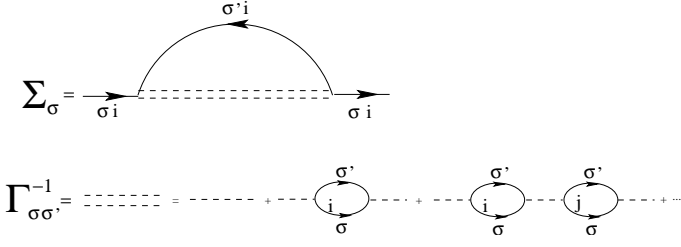


FIG. 3: Self-energy diagram $\Sigma_{\sigma\sigma'}$ to leading order in $1/N$.

T_τ is the time ordering operator with the imaginary time τ . As in the standard perturbation theory, we express the Green's function in term of its non-interacting form and the self-energy

$$G_\sigma^{-1}(\mathbf{k}, i\omega_n) = G_\sigma^{(0)-1}(\mathbf{k}, i\omega_n) - \Sigma_\sigma(\mathbf{k}, i\omega_n), \quad (6)$$

where $\Sigma_\sigma(\mathbf{k}, i\omega_n)$ is the (Matsubara) self-energy, $G_\sigma^{(0)}(\mathbf{k}, i\omega_n) = (i\omega_n - \varepsilon_{\sigma,\mathbf{k}} + \mu_\sigma)^{-1}$ is the bare Green's function, and $\varepsilon_{\sigma,\mathbf{k}} = \epsilon_{\mathbf{k}} + \bar{\omega}_\sigma$ is the bare fermionic dispersion.

The self-energy is determined to lowest order in $1/N$. It can be expressed as

$$\Sigma_\sigma(\mathbf{k}, i\omega_n) \equiv \sum_{\sigma'=1(\neq\sigma)}^3 \Sigma_{\sigma\sigma'}(\mathbf{k}, i\omega_n) \quad (7)$$

where $\Sigma_{\sigma\sigma'}$ is the self energy contribution of the level $|\sigma\rangle$ due to interactions with level $|\sigma'\rangle$, corresponding to the diagram of Fig. 3 and given by

$$\Sigma_{\sigma\sigma'}(\mathbf{k}, i\omega_n) = -\frac{1}{\beta N} \sum_{\Omega_m} \int \frac{d^3\mathbf{q}}{(2\pi)^3} \Gamma_{\sigma\sigma'}(\mathbf{q}, i\Omega_m) \quad (8)$$

$$\times G_{\sigma'}^{(0)}(\mathbf{q} - \mathbf{k}, i\Omega_m - i\omega_n).$$

The large- N renormalized interaction vertex (the T-matrix) is determined by $\Gamma_{\sigma\sigma'}^{-1}(\mathbf{q}, i\Omega_m) = -\frac{1}{\lambda_{\sigma\sigma'}} - \mathcal{C}_{\sigma\sigma'}(\mathbf{q}, i\Omega_m)$, where $\mathcal{C}_{\sigma\sigma'}(\mathbf{q}, i\Omega_m)$ is the correlator of the molecular (Cooper-pair) field operator $B_{\sigma\sigma'}(\mathbf{q}) = \int \frac{d^3\mathbf{p}}{(2\pi)^3} \psi_\sigma(\mathbf{p} + \mathbf{q})\psi_{\sigma'}(-\mathbf{p})$, that to leading order in $1/N$ is given by

$$\begin{aligned} \mathcal{C}_{\sigma\sigma'}(\mathbf{q}, i\Omega_m) &= \int_0^\beta d\tau e^{i\Omega_m\tau} \langle T_\tau \{ B_{\sigma\sigma'}(\mathbf{q}, \tau) B_{\sigma\sigma'}^\dagger(\mathbf{q}, 0) \} \rangle \\ &= \frac{1}{\beta} \sum_{\omega_n} \int \frac{d^3\mathbf{p}}{(2\pi)^3} G_\sigma^{(0)}(\mathbf{p} + \mathbf{q}, i\omega_n + i\Omega_m) G_{\sigma'}^{(0)}(-\mathbf{p}, -i\omega_n) \\ &= -\int \frac{d^3\mathbf{p}}{(2\pi)^3} \frac{1 - n_F(\xi_{\sigma,\mathbf{p}+}) - n_F(\xi_{\sigma',\mathbf{p}-})}{i\Omega_m - \xi_{\sigma,\mathbf{p}+} - \xi_{\sigma',\mathbf{p}-}}, \end{aligned} \quad (9)$$

and $\mathbf{p}_\pm = \mathbf{p} \pm \mathbf{q}/2$, $\xi_{\sigma,\mathbf{p}} = \varepsilon_{\sigma,\mathbf{p}} - \mu_\sigma$, $n_F(x) = 1/(e^{\beta x} + 1)$. An explicit expression for $\Gamma_{\sigma\sigma'}^{-1}(\mathbf{q}, \omega)$ at zero temperature may be found in the Appendix of Ref. 39.

For our analysis, we will need the retarded fermionic self-energy $\Sigma_{\sigma\sigma'}^R(\mathbf{k}, \omega)$ at real frequencies and at finite temperature. We denote with index R/A the retarded/advanced functions, *i.e.*, functions analytical in the upper/lower half-planes of the complex frequency. In some cases, it can be obtained directly from $\Sigma_{\sigma\sigma'}(\mathbf{k}, i\omega_n)$ via a replacement $i\omega_n \rightarrow \omega + i\delta$. However, in general it

is rather difficult to deal with discrete Matsubara sums. The approach we adopt here is to find the imaginary part of the retarded self-energy $\text{Im}[\Sigma_{\sigma\sigma'}^R(\mathbf{k}, \omega)]$ and obtain the real part via the Kramers-Kronig relation.

Applying a Lehmann spectral representation

$$f(i\omega_n) = \frac{1}{\pi} \int_{-\infty}^{\infty} dz \frac{\text{Im}[f^R(z)]}{z - i\omega_n}, \quad (10)$$

to (8), we find

$$\Sigma_{\sigma\sigma'}(\mathbf{k}, i\omega_n) = -\frac{4}{N\beta} \int \frac{d^3\mathbf{q}}{(2\pi)^3} \sum_{\Omega_m} \int_{-\infty}^{\infty} \frac{dz}{2\pi} \int_{-\infty}^{\infty} \frac{dz'}{2\pi} \text{Im}[\Gamma_{\sigma\sigma'}^R(\mathbf{q}, z)] \text{Im}[G_{\sigma'}^{R(0)}(\mathbf{q} - \mathbf{k}, z')] \times \frac{1}{z - i\Omega_m} \frac{1}{z' - i\Omega_m + i\omega_n} \quad (11)$$

After summing over the Matsubara frequencies Ω_m and performing the standard analytical continuation $i\omega_n \rightarrow \omega + i\delta$, we arrive to

$$\Sigma_{\sigma\sigma'}^R(\mathbf{k}, \omega) = -\frac{4}{N} \int \frac{d^3\mathbf{q}}{(2\pi)^3} \int_{-\infty}^{\infty} \frac{dz}{2\pi} \int_{-\infty}^{\infty} \frac{dz'}{2\pi} \frac{n_B(z) + n_F(z')}{z' - z + \omega + i\delta} \text{Im}[\Gamma_{\sigma\sigma'}^R(\mathbf{q}, z)] \text{Im}[G_{\sigma'}^{R(0)}(\mathbf{q} - \mathbf{k}, z')] \quad (12)$$

where $n_B(z) = \frac{1}{e^{\beta z} - 1}$. The imaginary part of this function can be obtained by performing the z' integral to obtain (denoting z by Ω)

$$\text{Im} [\Sigma_{\sigma\sigma'}^R(\mathbf{k}, \omega)] = \frac{2}{N} \int \frac{d^3\mathbf{q}}{(2\pi)^3} \int_{-\infty}^{\infty} \frac{d\Omega}{2\pi} \text{Im} [\Gamma_{\sigma\sigma'}^R(\mathbf{q}, \Omega)] \text{Im} [G_{\sigma'}^{R(0)}(\mathbf{q} - \mathbf{k}, \Omega - \omega)] [n_B(\Omega) + n_F(\Omega - \omega)]. \quad (13)$$

Using the Kramers-Kronig relation

$$\text{Re} [f(z)] = \frac{1}{\pi} \mathbb{P} \int_{-\infty}^{\infty} dz' \frac{\text{Im} [f(z')]}{z' - z} \quad (14)$$

we obtain the real part of the self energy

$$\begin{aligned} \text{Re} [\Sigma_{\sigma\sigma'}^R(\mathbf{k}, \omega)] = & \frac{2}{N} \int \frac{d^3\mathbf{q}}{(2\pi)^3} \int_{-\infty}^{\infty} \frac{d\Omega}{2\pi} \left[-\text{Im} [\Gamma_{\sigma\sigma'}^R(\mathbf{q}, \Omega)] \text{Re} [G_{\sigma'}^{R(0)}(\mathbf{q} - \mathbf{k}, \Omega - \omega)] n_B(\Omega) \right. \\ & \left. + \text{Re} [\Gamma_{\sigma\sigma'}^R(\mathbf{q}, \Omega)] \text{Im} [G_{\sigma'}^{R(0)}(\mathbf{q} - \mathbf{k}, \Omega - \omega)] n_F(\Omega - \omega) \right]. \end{aligned} \quad (15)$$

As mentioned in the Introduction, we are interested in the experimentally-relevant case where the number of atoms in each hyperfine state (species) is independently conserved. The Fermi wavevector $k_{F\sigma}$ for each hyperfine state is related to the corresponding density by the standard relation $n_\sigma = k_{F\sigma}^3/(6\pi^2)$. Since the atom densities are fixed at n_σ , the nontrivial self-energy corrections modify the dispersions and therefore lead to shifts in the chemical potentials μ_σ from their bare values of $\mu_{\sigma 0}$.

More specifically, the chemical potentials are determined by the condition $G^{-1}(k_{F\sigma}, \omega = 0) = 0$, yielding to lowest order in $1/N$ the relation

$$\begin{aligned} \mu_\sigma &= \mu_{\sigma 0} + \delta\mu_\sigma \\ \mu_{\sigma 0} &= \varepsilon_{\sigma, k_{F\sigma}} \\ \delta\mu_\sigma &= \text{Re} [\Sigma_\sigma(k_{F\sigma}, 0)]. \end{aligned} \quad (16)$$

where $\delta\mu_\sigma$ are the chemical potential shifts for states σ . At this point it is important to remark that although Eq. (16) is strictly a self-consistent equation, where μ_σ appears inside the self-energy, it would be overstepping the accuracy of the $1/N$ expansion to use anything other than the bare values $\mu_{\sigma 0}$ for the non-interacting Fermi gas at a particular polarization inside $\Sigma_{\sigma\sigma'}$.

Another quantity of interest is the two-particle correlation function

$$X_{\sigma\sigma'}(\mathbf{q}, i\nu_n) = - \int_0^\beta d\tau \int d^3\mathbf{r} e^{-i\mathbf{q}\cdot\mathbf{r} + i\nu_n\tau} \langle T_\tau \{ \psi_\sigma^\dagger(\mathbf{r}, \tau) \psi_{\sigma'}(\mathbf{r}, \tau) \psi_{\sigma'}^\dagger(0, 0) \psi_\sigma(0, 0) \} \rangle, \quad (17)$$

where $\nu_n = 2\pi n/\beta$ is the bosonic Matsubara frequency. To order $1/N$, we find for $\sigma \neq \sigma'$,

$$\begin{aligned} X_{\sigma\sigma'}(\mathbf{q}, i\nu_n) = & \frac{1}{\beta} \sum_m \int \frac{d^3\mathbf{k}}{(2\pi)^3} G_\sigma(\mathbf{k}, i\omega_m) G_{\sigma'}(\mathbf{k} + \mathbf{q}, i\omega_m + i\nu_n) \times \\ & \left[1 + \frac{1}{N} \frac{1}{\beta} \sum_\ell \int \frac{d^3\mathbf{k}'}{(2\pi)^3} G_\sigma(\mathbf{k}', i\omega'_\ell) G_{\sigma'}(\mathbf{k}' + \mathbf{q}, i\omega'_\ell + i\nu_n) \Gamma_{\sigma'\sigma}(\mathbf{k} + \mathbf{k}' + \mathbf{q}, i\omega_m + i\omega'_\ell + i\nu_n) \right], \end{aligned} \quad (18)$$

which, upon using a Lehmann spectral representation and analytic continuation to real frequencies becomes

$$\begin{aligned} X_{\sigma\sigma'}^R(\mathbf{q}, \nu) = & \int d\omega \int d\omega' \int \frac{d^3\mathbf{k}}{(2\pi)^3} A_\sigma(\mathbf{k}, \omega) A_{\sigma'}(\mathbf{k} + \mathbf{q}, \omega') \frac{n_F(\omega) - n_F(\omega')}{\nu + \omega - \omega' + i\delta} \\ & + \frac{1}{N} \int \left[\prod_{i=1}^5 dz_i \right] \int \frac{d^3\mathbf{k}}{(2\pi)^3} \int \frac{d^3\mathbf{k}'}{(2\pi)^3} A_\sigma(\mathbf{k}, z_1) A_{\sigma'}(\mathbf{k} + \mathbf{q}, z_2) A_\sigma(\mathbf{k}', z_3) A_{\sigma'}(\mathbf{k}' + \mathbf{q}, z_4) \frac{\text{Im} [\Gamma_{\sigma'\sigma}^R(\mathbf{k} + \mathbf{k}' + \mathbf{q}, z_5)]}{\pi} \times \\ & \frac{1}{z_2 - z_1 - \nu - i\delta} \frac{1}{z_4 - z_3 - \nu - i\delta} \left[\frac{n_{BF}(z_2, z_3, z_5)}{z_5 - z_2 - z_3} + \frac{n_{BF}(z_1, z_4, z_5)}{z_5 - z_1 - z_4} - \frac{n_{BF}(z_1, z_3, z_5)}{z_5 - z_1 - z_3 - \nu - i\delta} - \frac{n_{BF}(z_2, z_4, z_5)}{z_5 - z_2 - z_4 + \nu + i\delta} \right], \end{aligned} \quad (19)$$

where $n_{BF}(x, y, z) = [1 - n_F(x) - n_F(y)] n_B(z) - n_F(x)n_F(y)$, and

$$A_\sigma(\mathbf{k}, \omega) = -\frac{1}{\pi} \text{Im} [G_\sigma^R(\mathbf{k}, \omega)] \quad (20)$$

is the atomic spectral function.

We will be particularly interested in the case where the state $|3\rangle$ is empty, i.e., $k_{F3} = 0$. In this case, it is useful to parametrize the two remaining Fermi wavevector k_{F1} and k_{F2} in terms of the Fermi energy, ϵ_F , and the polarization, P . The Fermi energy is defined as $\epsilon_F = k_F^2/(2m)$, where $n = n_1 + n_2 \equiv k_F^3/(3\pi^2)$. The polarization, a measure of the population imbalance between states $|1\rangle$ and $|2\rangle$, is defined as

$$P \equiv \frac{n_1 - n_2}{n_1 + n_2} = \frac{(k_{F1})^3 - (k_{F2})^3}{(k_{F1})^3 + (k_{F2})^3} \quad (21)$$

The evaluation of Eq. (8) is meaningful until the condition $\Gamma_{\sigma\sigma'}^{-1}(\mathbf{q}, 0) > 0$ is violated for some \mathbf{q} , indicating an instability toward condensation of pairs with this momentum. At unitarity the instability in Γ_{12} occurs at polarization $P = 0.894(8)$, and $q = 0.773$. Although this is below the critical value $P_c = 0.93$ that follows from the mean field analysis, it should be remembered that the transition to the superfluid state is first order so that the lower value corresponds to a spinodal instability to some spatially inhomogeneous (FFLO) state [14, 15, 42, 43].

III. FERMION LIQUID PROPERTIES: SPECTRAL FUNCTION

One-particle quantities such as the momentum distributions $n_\sigma(\mathbf{k})$ are conveniently expressed in terms of the fermion spectral functions, $A_\sigma(\mathbf{k}, \omega)$, obtained from the retarded Green's function, Eq. 20. Note that in the case at hand, the medium and the interaction are isotropic and therefore the Green's function does not depend on the orientation of \mathbf{k} . We will therefore drop the vector notation for \mathbf{k} from now on. The momentum distribution, $n_\sigma(k)$ is then given by

$$n_\sigma(k) = \int_{-\infty}^{\infty} d\omega n_F(\omega) A_\sigma(k, \omega). \quad (22)$$

Near the Fermi surface, we can approximate the Green's function as a pole plus an incoherent spectrum

$$G_\sigma^R(k, \omega) = \frac{Z_\sigma}{\omega - E_\sigma(k) + i\gamma_\sigma(k)} + \dots, \quad (23)$$

where $E_\sigma(k)$ is the renormalized spectrum of excitations, $\gamma_\sigma(k)$ is the quasiparticle decay rate and Z_σ is the residue of the Green's function. This allows us to characterize the corresponding strongly-interacting normal state in terms of the Fermi liquid parameters. The renormalized spectrum is connected to the real part of the self energy through the relation

$$E_\sigma(k) = \varepsilon_{\sigma k} - \mu + \text{Re} [\Sigma_\sigma^R(k, E_\sigma(k))]. \quad (24)$$

The quasiparticle decay rate is given by $\gamma_\sigma(k) = -\text{Im} [\Sigma_\sigma^R(k, E_\sigma(k))]$, whereas the residue is given by

$$Z_\sigma = \left(1 - \frac{\partial}{\partial \omega} \text{Re} [\Sigma_\sigma^R(k_{F\sigma}, \omega)] \right)^{-1} \Big|_{\omega=0}. \quad (25)$$

The effective mass m_σ^* of the quasi particle at the Fermi surface is given by

$$\frac{m_\sigma^*}{m} = \frac{1}{Z_\sigma} \left(1 + \frac{m}{k} \frac{\partial}{\partial k} \text{Re} [\Sigma_\sigma^R(k, \omega)] \right)^{-1} \Big|_{k=k_{F\sigma}, \omega=0}. \quad (26)$$

We note that Eq. (8) coincides with the T-matrix approximation, and therefore will reproduce the known results in the dilute limit $na_{\sigma\sigma'}^3 \ll 1$ obtained from the pseudopotential $\frac{4\pi}{m} a_{\sigma\sigma'} \delta(\mathbf{r} - \mathbf{r}')$.

1. Numerical Results

For $P = 0.9$ at unitarity (i.e., $a_{12} = \infty$), the results for the majority ($|1\rangle$) and minority ($|2\rangle$) momentum distribution functions (Eq. 22) are shown in Fig. 1. The Migdal discontinuity at the Fermi wavevector is a measure of the quasiparticle residue and correspondingly are given by $Z_1 = 0.57$ and $Z_2 = 0.30$. An interesting feature of this distribution is that $n_2(0) \sim 0.45$, showing strong depletion (from the maximum value of 1) of the single-particle states down to zero momentum.

Quasiparticle properties, namely quasiparticle residues, effective masses and chemical potential shifts, are shown in Fig. 4. The properties are evaluated at large polarization $P \sim 0.9 - 1.0$ and for densities appropriate to ${}^6\text{Li}$ at the $B = 838$ G resonance. This corresponds to $a_{12} = \infty$, $a_{13} = -3288a_o$ and $a_{23} = -16080a_o$ where a_o is the Bohr radius ($a_o = 0.0529177\text{nm}$). In order to make contact with the experiment of Schunck *et al.* [19], we set the atomic density such that $k_F a_{13} = -3.3$ (which directly implies $k_F a_{23} = -16.1$). However, we stress that, given that the hyperfine state $|3\rangle$ is empty, the single particles properties of the hyperfine states $|1\rangle$ and $|2\rangle$ do not depend on the values of a_{23} and a_{13} . In this sense their properties are universal and our numerical result are applicable to other fermionic resonant atoms, e.g., ${}^{40}\text{K}$. On the other hand, the properties of the hyperfine state $|3\rangle$ are not universal in the sense that they depend on the interaction couplings.

Using the formula Eq. (25), we evaluate the quasiparticle residues Z_σ at zero temperature. At full polarization ($P = 1$), the residue $Z_1 = 1$ is maximum since the state $|2\rangle$ is empty. On the other hand, the residue $Z_2 = 0.47$ is much smaller than unity, indicating a large renormalization of atoms in state $|2\rangle$ due their interaction with atoms in state $|1\rangle$.

The binding energy of the minority carrier is $\mu_2 = -1.46\epsilon_F$, which can be compared to the Monte Carlo calculation of Ref. 28 that found $\mu_2 = -0.93\epsilon_F$.

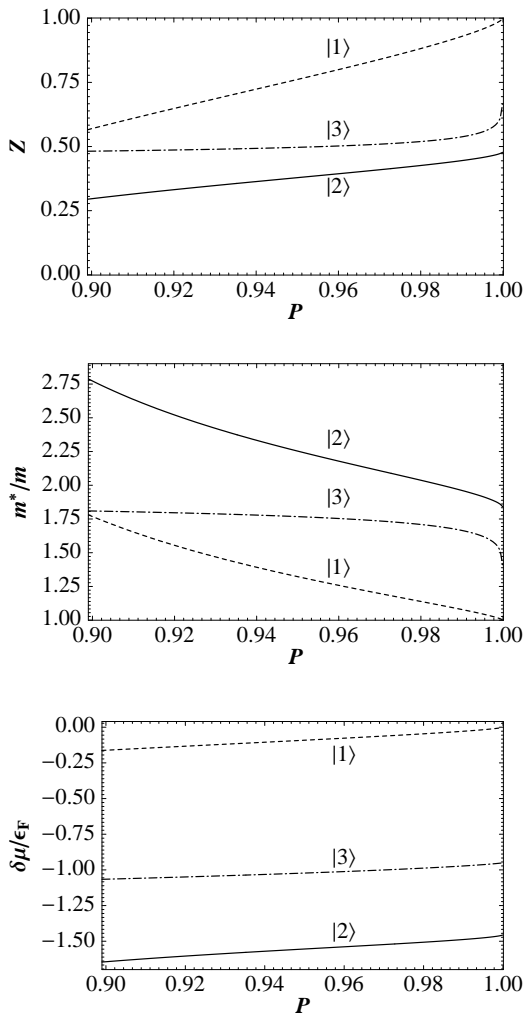


FIG. 4: Quasiparticle Fermi liquid properties:(A) residue Z_σ (Eq. 25), (B) effective mass m_σ^* (Eq. 26) and (C) the chemical potential shift $\delta\mu_\sigma$ (Eq. 16) of the hyperfine state |1) (dashed line), |2) (solid line) and |3) (dash-dotted line).

It is important to note here that previous computations [28] of the dispersion spectrum of the minority spin have all been done for the case of a single minority spin, in which case the problem is analogous to a Kondo/X-ray edge problem. Further, the dispersion spectrum is measured directly at $\mathbf{k} = 0$. In contrast, we are considering here the case of a finite density of minority spins, and the Fermi liquid properties near $k = k_{F2}$, with $|k - k_{F2}| \ll k_{F2}$. Even as $k_{F2} \rightarrow 0$, this regime is distinct from the single minority spin case. With unitary interactions, it is not clear how the two regimes will connect. We leave this important issue open for future work.

IV. RADIO FREQUENCY SPECTROSCOPY

We turn next to the RF spectroscopy of Refs. 5, 19. The RF spectroscopy is a technique used to probe atomic

correlation by exciting atoms from occupied hyperfine states to another (usually empty) reference hyperfine state. As we will see below, the RF probe provides valuable information about single particle excitations.

In the RF experiments of Schunck *et al.*, one focuses on three different atomic hyperfine states of the ^6Li atom. The two lowest states, |1) (majority) and |2) (minority), are populated and responsible for the superfluid correlations. The higher state, |3), is empty initially, and is used as a probe of atomic correlations in states |1) and |2). An RF field, at sufficiently large frequency, is used to drive atoms from state |2) to state |3).

In general the signal is expressed as a two-particle quantity. We calculate the rate for this process, described by a tunneling Hamiltonian that couples one of the species to a reference state |3) with a frequency ω detuned from the bare atomic transition.

The RF field induces a transition between atomic levels primarily through the electronic spin. In the AC field of interest, the rotating wave approximation is used to describe the tunneling Hamiltonian in terms of transfer matrix elements $V_{\mathbf{k},\mathbf{p}}$ between |2) to |3) state, i.e.,

$$\mathcal{H}_T = \int \frac{d^3\mathbf{k}}{(2\pi)^3} \frac{d^3\mathbf{p}}{(2\pi)^3} \left[V_{\mathbf{k}\mathbf{p}} e^{-i\omega_L t} \psi_3^\dagger(\mathbf{k}) \psi_2(\mathbf{p}) + h.c. \right] \quad (27)$$

For plane wave states, the tunneling matrix elements are $V_{\mathbf{k}\mathbf{p}} = \bar{V} (2\pi)^3 \delta(\mathbf{q}_L + \mathbf{k} - \mathbf{p})$. Here $q_L \approx 0$ and ω_L are the momentum and energy of the RF field. The conservation of momentum in tunneling is to be contrasted with the analogous Hamiltonian used to model tunneling in superconducting-metal junction.

The RF current is defined as $\hat{I}_3 = \dot{\hat{N}}_3 = i[\mathcal{H}_T, \hat{N}_3]$ where $\hat{N}_3 = \int d^3\mathbf{r} \psi_3^\dagger(\mathbf{r}) \psi_3(\mathbf{r})$ is the number operator of the hyperfine state |3). Thus the current operator is

$$\hat{I}_3(t) = -i\bar{V} \int \frac{d^3\mathbf{k}}{(2\pi)^3} \left[e^{-i\omega_L t} \psi_3^\dagger(\mathbf{k}) \psi_2(\mathbf{k}) - h.c. \right] \quad (28)$$

where as an accurate approximate we have neglected the extremely low RF photon momentum and set $\mathbf{q}_L = 0$. A standard linear response analysis gives

$$I_3(\nu) \equiv \langle \hat{I}_3(\nu) \rangle = 2\bar{V}^2 \text{Im} [X_{32}^R(\mathbf{0}, \nu)], \quad (29)$$

where $\nu = \omega_L + \bar{\omega}_2 - \bar{\omega}_3 - \mu_2 + \mu_3$ is the effective detuning. The retarded response function $X_{32}^R(\mathbf{0}, \nu)$ is obtained from the analytic continuation of Eq. 17, giving

$$\text{Im} [X_{32}^R(\mathbf{0}, \nu)] = \text{Im} [X_{32}^{(a)R}(\mathbf{0}, \nu)] + \text{Im} [X_{32}^{(b)R}(\mathbf{0}, \nu)], \quad (30)$$

where

$$\text{Im} \left[X_{\sigma\sigma'}^{(a)R}(\mathbf{0}, \nu) \right] = -\pi \int \frac{d^3\mathbf{k}}{(2\pi)^3} \int_{-\infty}^{\infty} d\omega [n_F(\omega) - n_F(\omega + \nu)] A_{\sigma}(\mathbf{k}, \omega) A_{\sigma'}(\mathbf{k}, \omega + \nu) \quad (31)$$

$$\begin{aligned} \text{Im} \left[X_{\sigma\sigma'}^{(b)R}(\mathbf{0}, \nu) \right] = & -\frac{\pi}{N} \int \frac{d^3\mathbf{k}}{(2\pi)^3} \int \frac{d^3\mathbf{k}'}{(2\pi)^3} \int_{-\infty}^{\infty} d\omega \int_{-\infty}^{\infty} d\omega' \times \\ & \left\{ -n_{BF}(\omega + \nu, \omega' + \nu, \omega + \omega' + \nu) G_{\sigma}(\mathbf{k}, \omega) A_{\sigma'}(\mathbf{k}, \omega + \nu) G_{\sigma}(\mathbf{k}', \omega') A_{\sigma'}(\mathbf{k}', \omega' + \nu) \Pi_{\sigma'\sigma}(\mathbf{k} + \mathbf{k}', \omega + \omega' + \nu) \right. \\ & + n_{BF}(\omega, \omega', \omega + \omega' + \nu) A_{\sigma}(\mathbf{k}, \omega) G_{\sigma'}(\mathbf{k}, \omega + \nu) A_{\sigma}(\mathbf{k}', \omega') G_{\sigma'}(\mathbf{k}', \omega' + \nu) \Pi_{\sigma'\sigma}(\mathbf{k} + \mathbf{k}', \omega + \omega' + \nu) \\ & + 2 [n_F(\omega) - n_F(\omega + \nu)] A_{\sigma}(\mathbf{k}, \omega) A_{\sigma'}(\mathbf{k}, \omega + \nu) \times \\ & \quad \left[n_B(\omega' + \omega + \nu) G_{\sigma}(\mathbf{k}', \omega') G_{\sigma'}(\mathbf{k}', \omega' + \nu) \Pi_{\sigma'\sigma}(\mathbf{k} + \mathbf{k}', \omega + \omega' + \nu) \right. \\ & \quad - n_F(\omega') A_{\sigma}(\mathbf{k}', \omega') G_{\sigma'}(\mathbf{k}', \omega' + \nu) \Gamma_{\sigma'\sigma}(\mathbf{k} + \mathbf{k}', \omega + \omega' + \nu) \\ & \quad \left. \left. - n_F(\omega' + \nu) G_{\sigma}(\mathbf{k}', \omega') A_{\sigma'}(\mathbf{k}', \omega' + \nu) \Gamma_{\sigma'\sigma}(\mathbf{k} + \mathbf{k}', \omega + \omega' + \nu) \right] \right\} \quad (32) \end{aligned}$$

where $\Pi_{\sigma\sigma'}(\mathbf{q}, \nu) = -\pi^{-1} \text{Im} [\Gamma_{\sigma\sigma'}(\mathbf{q}, \nu)]$.

An explicit expression for $\Gamma_{\sigma\sigma'}^{-1}(\mathbf{q}, \nu)$ at zero temperature may be found in the Appendix of Ref. 39. We note that in the limit of a vanishing interaction between states $|2\rangle$ and $|3\rangle$, i.e., for $a_{23} = 0$, there are no vertex corrections to the $X_{32}^R(\mathbf{0}, \nu)$ correlator, and we find

$$\begin{aligned} \text{Im} [X_{32}^R(\mathbf{0}, \nu)] &= \text{Im} [X_{32}^{(a)R}(\mathbf{0}, \nu)] \\ &= -\pi \int \frac{d^3\mathbf{k}}{(2\pi)^3} \int_{-\infty}^{\infty} d\omega [n_F(\omega) - n_F(\omega + \nu)] A_3(\mathbf{k}, \omega) A_2(\mathbf{k}, \omega + \nu), \quad (33) \end{aligned}$$

with all the interactions and corresponding $1/N$ corrections entering only through the atomic spectral functions $A_{2,3}(\mathbf{k}, \omega)$.

2. Numerical Results

We evaluate the RF spectrum for ${}^6\text{Li}$ at the resonance from the above expressions, displaying the result in Fig. 2. As we mentioned in the previous section, interactions between particles introduce self-energy corrections to the fermions. In the calculation of the RF spectrum, it is important to consider all scattering lengths because the spectral weight of the states $|2\rangle$ and $|3\rangle$ are affected by all interactions. Following the formula Eq. (31), we can evaluate the contribution $X_{32}^{(a)}(\mathbf{0}, \nu)$. We find that the bosonic propagators $\Gamma_{13}(\mathbf{q}, w)$ and $\Gamma_{23}(\mathbf{q}, w)$ have sharp poles at low momenta and positive energies. These positive energy ‘‘Aleiner-Altshuler’’ poles are analogous to the bifermion mode discussed in the context of weak superconductors above the paramagnetic limit [44]. The sharp poles provide an additional spectral weight of the states $|2\rangle$, $|3\rangle$ but are not found to be significant contributions given the large energy gap associated with these modes.

The interaction between states $|2\rangle$ and $|3\rangle$ introduces a vertex correction term, $X_{32}^{(b)}(\mathbf{0}, \nu)$, to the RF spectrum. Using the formula Eq. (32) and the condition that the reference state $|3\rangle$ is empty, we find that the vertex correction is not significant in the limit $P \sim 1$. For example, for polarization $P = 0.97$ the vertex correction is less than 0.1 %, as shown in Fig. 6.

In Figs. 5 and 2, we show the RF spectrum for the imbalanced polarization $P = 0.93$ and $P = 0.97$, respectively. Both RF signal peaks are positioned near $\Delta \sim 0.55 \epsilon_F$ which is nearly equal to the chemical potential difference between level $|2\rangle$ and $|3\rangle$ (see Fig. 4). The results for the peak position compare favorably to the recent MIT experiment of Schunck *et al.* [19] where they found $\Delta \sim 0.38 \epsilon_F$ at finite temperature $T/T_F \sim 0.08$. The position of the peak for $P = 0.93$ is closer to the non-interacting peak than $P = 0.97$ case, and the increased pairing fluctuations at $P = 0.93$ further broaden the linewidth.

V. CONCLUSION

We have studied the normal state of a resonantly interacting, three component Fermi gas at large population imbalance. To this end, we utilized a well-controlled large N (atom flavor) expansion, with $1/N$ as the small expansion parameter and showed that it provides a systematic way to treat the strong interactions characteristic of the unitary scattering point of a Feshbach resonant system. Although the accuracy of the $1/N$ expansion in the limit $N \rightarrow 1$ remains unproven in general, it has provided reasonable estimates in other settings. Our main aim was to provide a qualitative interpretation of recent RF experiments [19], and to emphasize the importance of mea-

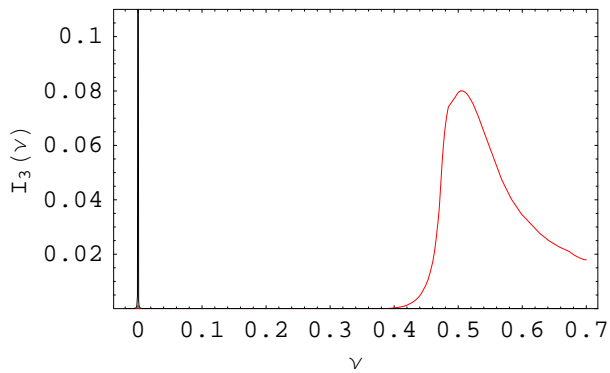


FIG. 5: RF spectrum for polarization $P = 0.93$: the intensity $I_3(\nu)$ (arbitrary units) vs. the detuning from the resonance frequency ν measured in units of the Fermi energy ϵ_F . The peak frequency relative to non-interacting line (black line) is smaller than for the $P = 0.97$ case shown in Fig. 2. The linewidth broadens for lower polarizations due to the increase in pairing fluctuations.

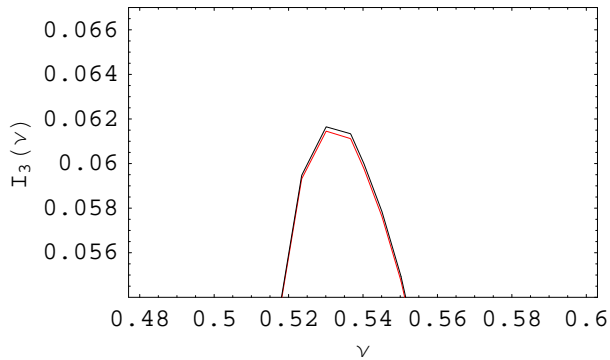


FIG. 6: Vertex correction to the RF spectrum for $P = 0.97$. The axes are the same as in Fig. 5. The red line includes the vertex correction, while the black line does not. The contribution of the correction $X_{32}^{(b)}(\mathbf{0}, \nu)$ is less than 0.1 %.

asuring quasiparticle properties to determine the nature of the ground state of imbalanced Fermi gases. Performing the analysis to leading order in $1/N$, we computed the atomic spectral functions and the momentum distribution functions with the characteristic Migdal discontinuity, thereby showing that the normal state is a conventional Fermi-liquid, albeit strongly renormalized. We then applied this formalism to analyze the RF excitation spectrum studied experimentally in Ref. 19. Our conclusion is that, indeed, the observed phenomenology can be well understood in terms of the strongly interacting, but conventional Fermi-liquid picture without resorting to exotic interpretations, such as, for example, pairing without condensation.

Note added: Recent experiments by the MIT group [45] have been interpreted in a physical picture consistent with that presented above, in contrast to their earlier interpretation of previous experiments [19].

Acknowledgments

We thank W. Ketterle and Y. Shin for useful discussions. This research was supported in part by the National Science Foundation under Grants No. DMR-0321848 (MV, DS, LR), DMR-0757145 (EGM,SS), and at the Kavli Institute for Theoretical Physics under grant PHY05-51164. EGM is also supported in part by the Samsung Scholarship.

-
- [1] C.A. Regal, M. Greiner, and D.S. Jin, Phys. Rev. Lett. **92**, 040403 (2004).
 [2] M.W. Zwierlein, C.A. Stan, C.H. Schunck, S.M.F. Raupach, A.J. Kerman, and W. Ketterle, Phys. Rev. Lett. **92**, 120403 (2004).
 [3] J. Kinast, S.L. Hemmer, M.E. Gehm, A. Turlapov, and J.E. Thomas, Phys. Rev. Lett. **92**, 150402 (2004).
 [4] T. Bourdel, L. Khaykovich, J. Cubizolles, J. Zhang, F. Chevy, M. Teichmann, L. Tarruell, S.J.J.M.F. Kokkelmans, and C. Salomon, Phys. Rev. Lett. **93**, 050401 (2004).
 [5] C. Chin, M. Bartenstein, A. Altmeyer, S. Riedl, S. Jochim, J.H. Denschlag, and R. Grimm, Science **305**, 1128 (2004).
 [6] M.W. Zwierlein, J.R. Abo-Shaeer, A. Schirotzek, C.H. Schunck, and W. Ketterle, Nature **435**, 1047 (2005).
 [7] Here we focus on the most experimentally relevant broad resonances. As discussed at length in Refs. 8, 9, in fact, for a narrow Feshbach resonance, there *is* a small physical parameter set by the ratio of the resonance width to Fermi energy, and therefore a full crossover can be described quantitatively via a controlled perturbation theory in this small parameter. Unfortunately, most experimentally studied Feshbach resonances are in fact broad, thus allowing only a *qualitative* description near the resonance (unitary point).
 [8] V. Gurarie, L. Radzihovsky and A.V. Andreev, Phys. Rev. Lett. **94**, 230403 (2005).
 [9] V. Gurarie and L. Radzihovsky, Annals of Physics **322**, 2 (2007).
 [10] G. B. Partridge, W. Li, R. I. Kamar, Y. Liao, and R. G. Hulet, Science **311**, 503 (2006).
 [11] M.W. Zwierlein, A. Schirotzek, C.H. Schunck, and W. Ketterle, Science **311**, 492 (2006).

- [12] G.B. Partridge, W. Li, Y. A. Liao, R. G. Hulet, M. Haque, and H.T.C. Stoof, *Phys. Rev. Lett.* **97**, 190407 (2006).
- [13] Y. Shin, M.W. Zwierlein, C.H. Schunck, A. Schirotzek, and W. Ketterle, *Phys. Rev. Lett.* **97**, 030401 (2006).
- [14] D.E. Sheehy and L. Radzihovsky, *Phys. Rev. Lett.* **96**, 060401 (2006).
- [15] D.E. Sheehy and L. Radzihovsky, *Annals of Physics* **322**, 1790 (2007).
- [16] P.F. Bedaque, H. Caldas, and G. Rupak, *Phys. Rev. Lett.* **91**, 247002 (2003).
- [17] M.W. Zwierlein, C.H. Schunck, A. Schirotzek, and W. Ketterle, *Nature* **442**, 54 (2006).
- [18] Even the extreme limit of a nearly fully polarized resonant gas, corresponding to a single minority fermionic atom resonantly interacting with a majority Fermi sea remains an open problem closely related to the X-ray edge singularity, as well as a mobility of an ionic impurity in metals.
- [19] C.H. Schunck, Y. Shin, A. Schirotzek, M. W. Zwierlein, and W. Ketterle, *Science* **316**, 867 (2007).
- [20] M. P. A. Fisher, P. B. Weichman, G. Grinstein, and D. S. Fisher, *Phys. Rev. B* **40**, 546 (1989).
- [21] M. Greiner, O. Mandel, T. Esslinger, T.W. Hansch, and I. Bloch, *Nature* **415**, 39 (2002).
- [22] J. Kinnunen, M. Rodriguez, and P. Torma, *Science* **305**, 1131 (2004).
- [23] Y. Ohashi and A. Griffin, *Phys. Rev. A* **72**, 013601 (2005).
- [24] Z. Yu and G. Baym, *Phys. Rev. A* **73**, 063601 (2006).
- [25] G. Baym, C. J. Pethick, Z. Yu, and M. W. Zwierlein, *Phys. Rev. Lett.* **99**, 190407 (2007).
- [26] S. Basu and E.J. Mueller, arXiv:0712.1007
- [27] Y. Shin, C. H. Schunck, A. Schirotzek, W. Ketterle *Phys. Rev. Lett.* **99**, 090403 (2007).
- [28] C. Lobo, A. Recati, S. Giorgini, and S. Stringari, *Phys. Rev. Lett.* **97**, 200403 (2006).
- [29] A. Bulgac and M.M. Forbes, *Phys. Rev. A* **75**, 031605(R) (2007).
- [30] J. Carlson and S. Reddy, *Phys. Rev. Lett.* **100**, 150403 (2008)
- [31] R. Combescot, A. Recati, C. Lobo, and F. Chevy, *Phys. Rev. Lett.* **98**, 180402 (2007).
- [32] M. Punk and W. Zwerger, *Phys. Rev. Lett.* **99**, 170404 (2007).
- [33] A. Perali, P. Pieri, G.C. Strinati, *Phys. Rev. Lett.* **100**, 010402 (2008).
- [34] Y. He, C.-C Chien, Q. Chen, and K. Levin, *Phys. Rev. A* **77**, 011602(R) (2008).
- [35] P. Massignan, G. M. Bruun, and H. T. C. Stoof, *Phys. Rev. A* **77**, 031601(R) (2008).
- [36] N. V. Prokof'ev and B. V. Svistunov, *Phys. Rev. B* **77**, 125101 (2008).
- [37] S. Powell, S. Sachdev, and H. P. Büchler, *Phys. Rev. B* **72**, 024534 (2005).
- [38] S. Sachdev and K. Yang, *Phys. Rev. B* **73**, 174504 (2006).
- [39] P. Nikolić and S. Sachdev, *Phys. Rev. A* **75**, 033608 (2007).
- [40] M. Y. Veillette, D. E. Sheehy, and L. Radzihovsky, *Phys. Rev. A* **75**, 043614 (2007).
- [41] C. A. Regal and D. S. Jin, *Phys. Rev. Lett.* **90**, 230404 (2003).
- [42] M.M. Parish, F.M. Marchetti, A. Lamacraft, and B.D. Simons, *Nat. Phys.* **3**, 124 (2007).
- [43] A. Lamacraft and F. M. Marchetti, *Phys. Rev. B* **77**, 014511 (2008).
- [44] I.L. Aleiner and B. L. Altshuler, *Phys. Rev. Lett.* **79**, 4242 (1997); F. Fumarola, I. L. Aleiner, and B. L. Altshuler, cond-mat/0703003.
- [45] C. H. Schunck, Y. Shin, A. Schirotzek, and W. Ketterle, *Nature* **454**, 739 (2008).